

Bose-Einstein correlations of three charged pions in hadronic Z^0 decays

The OPAL Collaboration

K. Ackerstaff⁸, G. Alexander²³, J. Allison¹⁶, N. Altekamp⁵, K.J. Anderson⁹, S. Anderson¹², S. Arcelli², S. Asai²⁴, S.F. Ashby¹, D. Axen²⁹, G. Azuelos^{18,a}, A.H. Ball¹⁷, E. Barberio⁸, R.J. Barlow¹⁶, R. Bartoldus³, J.R. Batley⁵, S. Baumann³, J. Bechtluft¹⁴, T. Behnke⁸, K.W. Bell²⁰, G. Bella²³, S. Bentvelsen⁸, S. Bethke¹⁴, S. Betts¹⁵, O. Biebel¹⁴, A. Biguzzi⁵, S.D. Bird¹⁶, V. Blobel²⁷, I.J. Bloodworth¹, M. Bobinski¹⁰, P. Bock¹¹, J. Böhme¹⁴, M. Boutemur³⁴, S. Braibant⁸, P. Bright-Thomas¹, R.M. Brown²⁰, H.J. Burckhart⁸, C. Burgard⁸, R. Bürgin¹⁰, P. Capiluppi², R.K. Carnegie⁶, A.A. Carter¹³, J.R. Carter⁵, C.Y. Chang¹⁷, D.G. Charlton^{1,b}, D. Chrisman⁴, C. Ciocca², P.E.L. Clarke¹⁵, E. Clay¹⁵, I. Cohen²³, J.E. Conboy¹⁵, O.C. Cooke⁸, C. Couyoumtzelis¹³, R.L. Coxe⁹, M. Cuffiani², S. Dado²², G.M. Dallavalle², R. Davis³⁰, S. De Jong¹², L.A. del Pozo⁴, A. de Roeck⁸, K. Desch⁸, B. Dienes^{33,d}, M.S. Dixit⁷, M. Doucet¹⁸, J. Dubbert³⁴, E. Duchovni²⁶, G. Duckeck³⁴, I.P. Duerdoth¹⁶, D. Eatough¹⁶, P.G. Estabrooks⁶, E. Etzion²³, H.G. Evans⁹, F. Fabbri², A. Fanfani², M. Fanti², A.A. Faust³⁰, F. Fiedler²⁷, M. Fierro², H.M. Fischer³, I. Fleck⁸, R. Folman²⁶, A. Fürties⁸, D.I. Futyan¹⁶, P. Gagnon⁷, J.W. Gary⁴, J. Gascon¹⁸, S.M. Gascon-Shotkin¹⁷, C. Geich-Gimbel³, T. Geralis²⁰, G. Giacomelli², P. Giacomelli², V. Gibson⁵, W.R. Gibson¹³, D.M. Gingrich^{30,a}, D. Glenzinski⁹, J. Goldberg²², W. Gorn⁴, C. Grandi², E. Gross²⁶, J. Grunhaus²³, M. Gruwe²⁷, G.G. Hanson¹², M. Hansroul⁸, M. Hapke¹³, C.K. Hargrove⁷, C. Hartmann³, M. Hauschild⁸, C.M. Hawkes⁵, R. Hawkings²⁷, R.J. Hemingway⁶, M. Herndon¹⁷, G. Herten¹⁰, R.D. Heuer⁸, M.D. Hildreth⁸, J.C. Hill⁵, S.J. Hillier¹, P.R. Hobson²⁵, A. Hocker⁹, R.J. Homer¹, A.K. Honma^{28,a}, D. Horváth^{32,c}, K.R. Hossain³⁰, R. Howard²⁹, P. Hüntemeyer²⁷, P. Igo-Kemenes¹¹, D.C. Imrie²⁵, K. Ishii²⁴, F.R. Jacob²⁰, A. Jawahery¹⁷, H. Jeremie¹⁸, M. Jimack¹, A. Joly¹⁸, C.R. Jones⁵, P. Jovanovic¹, T.R. Junk⁸, D. Karlen⁶, V. Kartvelishvili¹⁶, K. Kawagoe²⁴, T. Kawamoto²⁴, P.I. Kayal³⁰, R.K. Keeler²⁸, R.G. Kellogg¹⁷, B.W. Kennedy²⁰, A. Klier²⁶, S. Kluth⁸, T. Kobayashi²⁴, M. Kobel^{3,e}, D.S. Koetke⁶, T.P. Kokott³, M. Kolrep¹⁰, S. Komamiya²⁴, R.V. Kowalewski²⁸, T. Kress¹¹, P. Krieger⁶, J. von Krogh¹¹, P. Kyberd¹³, G.D. Lafferty¹⁶, D. Lanske¹⁴, J. Lauber¹⁵, S.R. Lautenschlager³¹, I. Lawson²⁸, J.G. Layter⁴, D. Lazic²², A.M. Lee³¹, E. Lefebvre¹⁸, D. Lellouch²⁶, J. Letts¹², L. Levinson²⁶, R. Liebisch¹¹, B. List⁸, C. Littlewood⁵, A.W. Lloyd¹, S.L. Lloyd¹⁶, F.K. Loebinger¹⁶, G.D. Long²⁸, M.J. Losty⁷, J. Ludwig¹⁰, D. Lui¹², A. Macchiolo², A. Macpherson³⁰, M. Mannelli⁸, S. Marcellini², C. Markopoulos¹³, A.J. Martin¹³, J.P. Martin¹⁸, G. Martinez¹⁷, T. Mashimo²⁴, P. Mättig²⁶, W.J. McDonald³⁰, J. McKenna²⁹, E.A. Mckigney¹⁵, T.J. McMahon¹, R.A. McPherson²⁸, F. Meijers⁸, S. Menke³, F.S. Merritt⁹, H. Mes⁷, J. Meyer²⁷, A. Michelini², S. Mihara²⁴, G. Mikenberg²⁶, D.J. Miller¹⁵, R. Mir²⁶, W. Mohr¹⁰, A. Montanari², T. Mori²⁴, K. Nagai²⁶, I. Nakamura²⁴, H.A. Neal¹², B. Nellen³, R. Nisius⁸, S.W. O’Neale¹, F.G. Oakham⁷, F. Odoricci², H.O. Ogren¹², M.J. Oreglia⁹, S. Orito²⁴, J. Pálinkás^{33,d}, G. Pásztor³², J.R. Pater¹⁶, G.N. Patrick²⁰, J. Patt¹⁰, R. Perez-Ochoa⁸, S. Petzold²⁷, P. Pfeifenschneider¹⁴, J.E. Pilcher⁹, J. Pinfold³⁰, D.E. Plane⁸, P. Poffenberger²⁸, B. Poli², J. Polok⁸, M. Przybycien⁸, C. Rembser⁸, H. Rick⁸, S. Robertson²⁸, S.A. Robins²², N. Rodning³⁰, J.M. Roney²⁸, K. Roscoe¹⁶, A.M. Rossi², Y. Rozen²², K. Runge¹⁰, O. Runolfsson⁸, D.R. Rust¹², K. Sachs¹⁰, T. Saeki²⁴, O. Sahr³⁴, W.M. Sang²⁵, E.K.G. Sarkisyan²³, C. Sbarra²⁹, A.D. Schaile³⁴, O. Schaile³⁴, F. Scharf³, P. Scharff-Hansen⁸, J. Schieck¹¹, B. Schmitt⁸, S. Schmitt¹¹, A. Schöning⁸, T. Schorner³⁴, M. Schröder⁸, M. Schumacher³, C. Schwick⁸, W.G. Scott²⁰, R. Seuster¹⁴, T.G. Shears⁸, B.C. Shen⁴, C.H. Shepherd-Themistocleous⁸, P. Sherwood¹⁵, G.P. Siroli², A. Sittler²⁷, A. Skuja¹⁷, A.M. Smith⁸, G.A. Snow¹⁷, R. Sobie²⁸, S. Söldner-Rembold¹⁰, M. Sproston²⁰, A. Stahl³, K. Stephens¹⁶, J. Steuerer²⁷, K. Stoll¹⁰, D. Strom¹⁹, R. Ströhmer³⁴, R. Tafirout¹⁸, S.D. Talbot¹, S. Tanaka²⁴, P. Taras¹⁸, S. Tarem²², R. Teuscher⁸, M. Thiergen¹⁰, M.A. Thomson⁸, E. von Törne³, E. Torrence⁸, S. Towers⁶, I. Trigger¹⁸, Z. Trócsányi³³, E. Tsur²³, A.S. Turcot⁹, M.F. Turner-Watson⁸, R. Van Kooten¹⁰, P. Vannerem¹⁰, M. Verzocchi¹⁰, P. Vikas¹⁸, H. Voss³, F. Wackerle¹⁰, A. Wagner²⁷, C.P. Ward⁵, D.R. Ward⁵, P.M. Watkins¹, A.T. Watson¹, N.K. Watson¹, P.S. Wells⁸, N. Wermes³, J.S. White²⁸, G.W. Wilson¹⁴, J.A. Wilson¹, T.R. Wyatt¹⁶, S. Yamashita²⁴, G. Yekutieli²⁶, V. Zacek¹⁸, D. Zer-Zion⁸

¹ School of Physics and Astronomy, University of Birmingham, Birmingham B15 2TT, UK

² Dipartimento di Fisica dell’ Università di Bologna and INFN, I-40126 Bologna, Italy

³ Physikalisches Institut, Universität Bonn, D-53115 Bonn, Germany

⁴ Department of Physics, University of California, Riverside CA 92521, USA

⁵ Cavendish Laboratory, Cambridge CB3 0HE, UK

⁶ Ottawa-Carleton Institute for Physics, Department of Physics, Carleton University, Ottawa, Ontario K1S 5B6, Canada

- ⁷ Centre for Research in Particle Physics, Carleton University, Ottawa, Ontario K1S 5B6, Canada
⁸ CERN, European Organisation for Particle Physics, CH-1211 Geneva 23, Switzerland
⁹ Enrico Fermi Institute and Department of Physics, University of Chicago, Chicago IL 60637, USA
¹⁰ Fakultät für Physik, Albert Ludwigs Universität, D-79104 Freiburg, Germany
¹¹ Physikalisches Institut, Universität Heidelberg, D-69120 Heidelberg, Germany
¹² Indiana University, Department of Physics, Swain Hall West 117, Bloomington IN 47405, USA
¹³ Queen Mary and Westfield College, University of London, London E1 4NS, UK
¹⁴ Technische Hochschule Aachen, III Physikalisches Institut, Sommerfeldstrasse 26-28, D-52056 Aachen, Germany
¹⁵ University College London, London WC1E 6BT, UK
¹⁶ Department of Physics, Schuster Laboratory, The University, Manchester M13 9PL, UK
¹⁷ Department of Physics, University of Maryland, College Park, MD 20742, USA
¹⁸ Laboratoire de Physique Nucléaire, Université de Montréal, Montréal, Quebec H3C 3J7, Canada
¹⁹ University of Oregon, Department of Physics, Eugene OR 97403, USA
²⁰ Rutherford Appleton Laboratory, Chilton, Didcot, Oxfordshire OX11 0QX, UK
²² Department of Physics, Technion-Israel Institute of Technology, Haifa 32000, Israel
²³ Department of Physics and Astronomy, Tel Aviv University, Tel Aviv 69978, Israel
²⁴ International Centre for Elementary Particle Physics and Department of Physics, University of Tokyo, Tokyo 113, and Kobe University, Kobe 657, Japan
²⁵ Institute of Physical and Environmental Sciences, Brunel University, Uxbridge, Middlesex UB8 3PH, UK
²⁶ Particle Physics Department, Weizmann Institute of Science, Rehovot 76100, Israel
²⁷ Universität Hamburg/DESY, II Institut für Experimental Physik, Notkestrasse 85, D-22607 Hamburg, Germany
²⁸ University of Victoria, Department of Physics, P O Box 3055, Victoria BC V8W 3P6, Canada
²⁹ University of British Columbia, Department of Physics, Vancouver BC V6T 1Z1, Canada
³⁰ University of Alberta, Department of Physics, Edmonton AB T6G 2J1, Canada
³¹ Duke University, Dept of Physics, Durham, NC 27708-0305, USA
³² Research Institute for Particle and Nuclear Physics, H-1525 Budapest, P O Box 49, Hungary
³³ Institute of Nuclear Research, H-4001 Debrecen, P O Box 51, Hungary
³⁴ Ludwigs-Maximilians-Universität München, Sektion Physik, Am Coulombwall 1, D-85748 Garching, Germany

Received: 7 May 1998 / Published online: 12 August 1998

Abstract. Bose-Einstein Correlations (BEC) of three identical charged pions were studied in 4×10^6 hadronic Z^0 decays recorded with the OPAL detector at LEP. The genuine three-pion correlations, corrected for the Coulomb effect, were separated from the known two-pion correlations by a new subtraction procedure. A significant genuine three-pion BEC enhancement near threshold was observed having an emitter source radius of $r_3 = 0.580 \pm 0.004$ (stat.) ± 0.029 (syst.) fm and a strength of $\lambda_3 = 0.504 \pm 0.010$ (stat.) ± 0.041 (syst.). The Coulomb correction was found to increase the λ_3 value by $\sim 9\%$ and to reduce r_3 by $\sim 6\%$. The measured λ_3 corresponds to a value of 0.707 ± 0.014 (stat.) ± 0.078 (syst.) when one takes into account the three-pion sample purity. A relation between the two-pion and the three-pion source parameters is discussed.

1 Introduction

Bose-Einstein Correlations (BEC) between pairs of identical bosons, mainly the $\pi^\pm\pi^\pm$ system, have been extensively studied in a large variety of interactions and over a wide range of energies [1,2]. These correlations, which are present when the bosons are near to one another in phase space, are used to estimate the size of the emitter of the particles and more recently in QCD-based models to describe fragmentation and hadronisation in high energy reactions [3,4]. The two-pion BEC effect has lately also been discussed [5] in connection with the measurement of

the W mass in the reaction $e^+e^- \rightarrow W^+W^- \rightarrow \text{hadrons}$ at LEP2.

In systems of more than two identical bosons, BEC are also expected to be present. These higher-order correlations may affect the multi-hadron production and are also of interest in intermittency studies [6]. Detection of the “genuine” multi-boson BEC is complicated by the fact that they have to be isolated from the lower-order boson correlations and therefore require large data samples. In addition, systems of several identical charged bosons, placed nearby in phase space, are subject to a relatively large repulsive Coulomb interaction which may suppress the BEC effect. As a consequence, only relatively few higher order BEC studies of three and more charged pions have been reported [7–13]. In those studies, mainly due to lack of statistics, it was not possible to isolate and verify the genuine multi-boson BEC from the lower-order ones. Attempts have been made to infer from the measured BEC of the multi-boson systems the individual con-

^a and at TRIUMF, Vancouver, Canada V6T 2A3

^b and Royal Society University Research Fellow

^c and Institute of Nuclear Research, Debrecen, Hungary

^d and Department of Experimental Physics, Lajos Kossuth University, Debrecen, Hungary

^e on leave of absence from the University of Freiburg

tribution of each of the higher order correlations by model dependent formulae. A significant genuine BEC signal of three identical charged pions, $\pi^\pm\pi^\pm\pi^\pm$, has been reported in a hadron-proton interaction experiment [12] and more recently in a LEP experiment [13] where, however, the Coulomb effect was neglected.

Here we report on a BEC study of the $\pi^\pm\pi^\pm\pi^\pm$ system carried out with a large sample of approximately 4×10^6 hadronic Z^0 decays, recorded by the OPAL detector at the e^+e^- LEP collider during the years 1991 to 1995. In this analysis, which takes into account the Coulomb effect, we have isolated the genuine three-pion BEC and estimated the size of the emitter. In Sect. 2 we introduce the extension of the two-boson BEC to the system of three identical bosons. Section 3 is devoted to the procedure used for the Coulomb correction of the three-pion BEC and in Sect. 4 the experimental details are given. In Sect. 5 we describe our method for the extraction of the genuine $\pi^\pm\pi^\pm\pi^\pm$ BEC and present the results obtained from our analysis. The relations between the two-pion and the genuine three-pion BEC parameters are explored in Sect. 6. Finally, the summary and conclusions are presented in Sect. 7.

2 The three-boson correlation function

In describing the three-boson BEC we follow the approach which was also adopted, for example, in [2]. The BEC of pairs of identical bosons can be formally expressed in terms of the normalised function

$$R_2 = \frac{\rho_2(p_1, p_2)}{\rho_1(p_1)\rho_1(p_2)} = \sigma \frac{d^2\sigma}{dp_1 dp_2} / \left\{ \frac{d\sigma}{dp_1} \frac{d\sigma}{dp_2} \right\}, \quad (1)$$

where σ is the total boson production cross section, $\rho_1(p_i)$ and $d\sigma/dp_i$ are the single-boson density in momentum space and the inclusive cross section, respectively. Similarly $\rho_2(p_1, p_2)$ and $d^2\sigma/dp_1 dp_2$ are respectively the density of the two-boson system and its inclusive cross section. The product of the independent one-particle densities $\rho_1(p_1)\rho_1(p_2)$ is referred to as the reference density distribution, or reference sample, to which the measured correlations are compared. The inclusive two-boson density $\rho_2(p_1, p_2)$ can be written as:

$$\rho_2(p_1, p_2) = \rho_1(p_1)\rho_1(p_2) + K_2(p_1, p_2), \quad (2)$$

where $K_2(p_1, p_2)$ represents the two-body correlations. In the simple case of two identical bosons the normalised density function R_2 , defined in (1), already describes the genuine two-body correlations and has been referred to in previous BEC studies of OPAL [14, 15] as the C_2 correlation function. Thus one has

$$C_2 \equiv R_2 = 1 + \tilde{K}_2(p_1, p_2), \quad (3)$$

where $\tilde{K}_2(p_1, p_2) = K_2(p_1, p_2)/[\rho_1(p_1)\rho_1(p_2)]$ is the normalised two-body correlation term. Since Bose-Einstein correlation are present when the bosons are close to one

another in phase space, one natural choice is to study them as a function of the variable Q_2 defined by

$$Q_2^2 = q_{1,2}^2 = -(p_1 - p_2)^2 = M_2^2 - 4\mu^2,$$

which approaches zero as the identical bosons move closer in phase space. Here p_i is the four-momentum vector of the i th particle, μ is the boson mass and M_2^2 is the invariant mass squared of the two-boson system.

In the parametrisation proposed by Goldhaber et al. [16], C_2 has the form

$$C_2(Q_2) = 1 + \lambda_2 e^{-Q_2^2/r_2^2}, \quad (4)$$

where r_2 estimates the size of the two-boson emitter which is taken to be of Gaussian shape. The strength of the BEC effect, frequently referred to as the chaoticity parameter, is measured by λ_2 which varies in the range $0 \leq \lambda_2 \leq 1$.

The inclusive density of three bosons, $\rho_3(p_1, p_2, p_3)$, includes the three independent boson momentum spectra, the two-particle correlations K_2 and the genuine three-particle correlations K_3 , namely:

$$\rho_3(p_1, p_2, p_3) = \rho_1(p_1)\rho_1(p_2)\rho_1(p_3) + \sum_{(3)} \rho_1(p_i)K_2(p_j, p_k) + K_3(p_1, p_2, p_3), \quad (5)$$

where the summation is taken over all the three possible permutations. The normalised inclusive three-body density, is then given by

$$R_3 = \frac{\rho_3(p_1, p_2, p_3)}{\rho_1(p_1)\rho_1(p_2)\rho_1(p_3)} = 1 + R_{1,2} + \tilde{K}_3(p_1, p_2, p_3). \quad (6)$$

Here

$$R_{1,2} = \frac{\sum_{(3)} \rho_1(p_i)K_2(p_j, p_k)}{\rho_1(p_1)\rho_1(p_2)\rho_1(p_3)}, \quad (7)$$

represents a mixed three-boson system in which only two of them are correlated, and

$$\tilde{K}_3(p_1, p_2, p_3) = \frac{K_3(p_1, p_2, p_3)}{\rho_1(p_1)\rho_1(p_2)\rho_1(p_3)}, \quad (8)$$

represents the three-boson correlation. In analogy with C_2 , one can define a correlation function C_3 , which measures the genuine three-boson correlation, by subtracting from R_3 the term which contains the two-boson correlations contribution. Thus

$$C_3 \equiv R_3 - R_{1,2} = 1 + \tilde{K}_3(p_1, p_2, p_3), \quad (9)$$

which depends only on the genuine three-boson correlations. For the study of the three-boson correlations we use the variable Q_3 which is defined as

$$Q_3^2 = \sum_{(3)} q_{i,j}^2 = M_3^2 - 9\mu^2,$$

where the summation is taken over all the three different i, j boson pairs and M_3^2 is the invariant mass squared of the three-boson system. From the definition of this three-boson variable it is clear that as Q_3 approaches zero so do the three $q_{i,j}$ values which eventually reach the region where the two-boson BEC enhancement is observed.

The genuine three-pion correlation function $C_3(Q_3)$ can be parametrised by the expression [9]

$$C_3(Q_3) = 1 + 2\lambda_3 e^{-Q_3^2 r_3^2}, \quad (10)$$

where λ_3 , which can vary within the limits $0 \leq \lambda_3 \leq 1$, measures the strength of the three-boson BEC effect and r_3 estimates the size of the three-boson emitter. The factor two which multiplies λ_3 arises from the presence of two possible diagrams with exchange of all the identical pions within a triplet. To extract from the data values for the strength λ_3 and the emitter size r_3 , we modified (10) to read

$$C_3(Q_3) = \kappa(1 + 2\lambda_3 e^{-Q_3^2 r_3^2})(1 + \varepsilon Q_3), \quad (11)$$

where κ is a normalisation factor and the linear term $(1 + \varepsilon Q_3)$ accounts for the long range correlations arising from charge and energy conservation and phase space constraints. Higher-order Q_3 terms for the long range correlations were found not to be needed in the present analysis.

3 The Coulomb correction

The observed BEC of identical charged bosons is suppressed by the Coulomb repulsive force. To account for this effect a correction to the measured BEC distribution is required. If $C_2(Q_2)$ is the two-boson correlation in the presence of the Coulomb effect then it is related to the true $C_2^{\text{true}}(Q_2)$ through the function $G_2(Q_2)$, so that

$$C_2(Q_2) = G_2(Q_2) C_2^{\text{true}}(Q_2). \quad (12)$$

In the case that the reference sample is a Monte Carlo generated data without the Coulomb effect, $G_2(Q_2)$ can be expressed by the Gamow factor [17]:

$$G_2(Q_2) = 2\pi\eta / (e^{2\pi\eta} - 1), \quad (13)$$

where $\eta = \alpha_{\text{em}} e_1 e_2 \mu / Q_2$. Here e_1 and e_2 are the charges, in positron units, of the two bosons having a mass of μ , and α_{em} is the fine-structure constant. Recently alternative Coulomb corrections [18,19] for the two-boson system have been proposed, which are based on non-Gaussian parametrisations. These could not be extended to the three-pion system and therefore were not used in our analysis.

For a given three charged bosons system, with boson pairs having Q_2 values of $q_{1,2}$, $q_{1,3}$ and $q_{2,3}$, the Coulomb correction G_3 can be approximated, in terms of the G_2 function by [9]:

$$G_3(Q_3) = \langle G_2(q_{1,2}) G_2(q_{2,3}) G_2(q_{1,3}) \rangle, \quad (14)$$

where the average is taken over all experimentally accessible values of $q_{i,j}$ which satisfy the condition $Q_3^2 = \sum_{(3)} q_{i,j}^2$.

The function $G_3(Q_3)$ can be evaluated through (14) or by using a slightly more precise formulation proposed in [20]. In our analysis the differences between the results of these two methods were smaller than the statistical errors so that the simpler method was sufficiently accurate for our purposes.

4 Experimental setup and data selection

4.1 The OPAL detector

Details of the OPAL detector and its performance at the LEP e^+e^- collider are given elsewhere [21]. Here we will describe briefly only those detector components pertinent to the present analysis, namely the central tracking chambers.

Besides a silicon microvertex detector, the central tracking chambers consist of a precision vertex detector, a large jet chamber, and additional z -chambers surrounding the jet chamber. The vertex detector is a 1 m long, two-layer cylindrical drift chamber that surrounds the beam pipe¹. The jet chamber has a length of 4 m and a diameter of 3.7 m. It is divided into 24 sectors in ϕ , each equipped with 159 sense wires parallel to the beam ensuring a large number of measured points even for particles emerging from a secondary vertex. The jet chamber also provides a measurement of the specific energy loss, dE/dx , of charged particles [22]. A resolution of 3–4% on dE/dx has been obtained, allowing particle identification over a large momentum range. The z -chambers, 4 m long, 50 cm wide and 59 mm thick, allow a precise measurement of the z -coordinate of the charged tracks. They cover polar angles in the region $|\cos(\theta)| \leq 0.72$ and 94% of the azimuthal angular range. All the chambers are contained in a solenoid providing an axial magnetic field of 0.435 T. The combination of these chambers leads to a momentum resolution of $\sigma_{p_t}/p_t \approx \sqrt{(0.02)^2 + (0.0015 \cdot p_t)^2}$, where p_t in GeV/ c is the transverse momentum with respect to the beam direction. The first term under the square root sign represents the contribution from multiple Coulomb scattering [23].

4.2 Data selection

The analysis was performed with the OPAL data collected at LEP with centre of mass energies on and around the Z^0 peak with the requirement that the jet and z -chambers were fully operational. The hadronic Z^0 decays were selected according to the number of charged tracks and the visible energy of the event [24]. We applied the same

¹ A right-handed coordinate system is adopted by OPAL, where the x -axis points to the centre of the LEP ring, and positive z is along the electron beam direction. The angles θ and ϕ are the polar and azimuthal angles respectively

track quality and dE/dx cuts described in a former OPAL BEC study of two identical charged pions [14]. Furthermore, events with a thrust angle of $|\cos(\theta_{\text{thrust}})| > 0.82$ with respect to the beam axis were rejected. Finally we accepted only events with a relative charge balance of $|(n^+ - n^-)/(n^+ + n^-)| < 0.25$, where n^+ and n^- are respectively the observed numbers of positively and negatively charged tracks. Following these criteria a total of 2.65×10^6 hadronic Z^0 decay events were used in the analysis.

To avoid configurations with overlapping tracks, we rejected pion pairs if their invariant mass was less than 0.4 GeV and if the opening angle between them in the plane perpendicular to the beam axis was less than 0.05 rad. In the present analysis all charged tracks are assumed to be pions. From Monte Carlo (MC) studies [24] we have estimated that the average pion purity of our charged track sample is 89.3% with a systematic uncertainty of $\pm 2.2\%$ and a negligible statistical error. Thus the pion purity of the three charged track system is $71.3 \pm 5.3\%$.

5 Analysis and results

The BEC analysis used the hadronic Z^0 decay data of OPAL where in each event all possible $\pi^\pm\pi^\pm\pi^\pm$ combinations were taken as the data sample. For the reference distribution we used a Monte Carlo generated sample [25] of 4×10^6 JETSET 7.4 events which have passed a full detector simulation [26] but do not include BEC and Coulomb effects. This JETSET Monte Carlo program, which includes most of the known resonances which decay into the $\pi^+\pi^-$ and $\pi^\pm\pi^\pm\pi^\mp$ final states, was carefully tuned to the OPAL data [27]. Here one should note that the $\pi^\pm\pi^\pm\pi^\mp$ systems of the measured data contain one pair of identical pions and therefore cannot be used as a reference sample. Thus:

$$R_3(Q_3) = \frac{N^{\pm\pm\pm}(Q_3)}{M^{\pm\pm\pm}(Q_3)}, \quad (15)$$

where $N^{\pm\pm\pm}(Q_3)$ is the number of the $\pi^\pm\pi^\pm\pi^\pm$ data combinations and $M^{\pm\pm\pm}(Q_3)$ is the corresponding number of Monte Carlo $\pi^\pm\pi^\pm\pi^\pm$ combinations at the same Q_3 value. The Monte Carlo sample was normalised to the data in a Q_3 region far away from any observable BEC enhancement. This was achieved by requiring that the integrated number of the Monte Carlo entries in the Q_3 range 1.6 – 2.0 GeV was equal to that of the data. The measured $R_3(Q_3)$ distribution is shown in Fig. 1a in the range of $0.2 < Q_3 < 2.0$ GeV. The data points below 0.25 GeV have relatively large errors, and a lower three-track separation efficiency of identical charged tracks. Therefore a lower limit of 0.25 GeV was imposed on the analysis. In the figure a clear enhancement is observed in the region below $Q_3 = 1$ GeV. This enhancement can be interpreted as coming from both the known two-pion and from the genuine three-pion BEC.

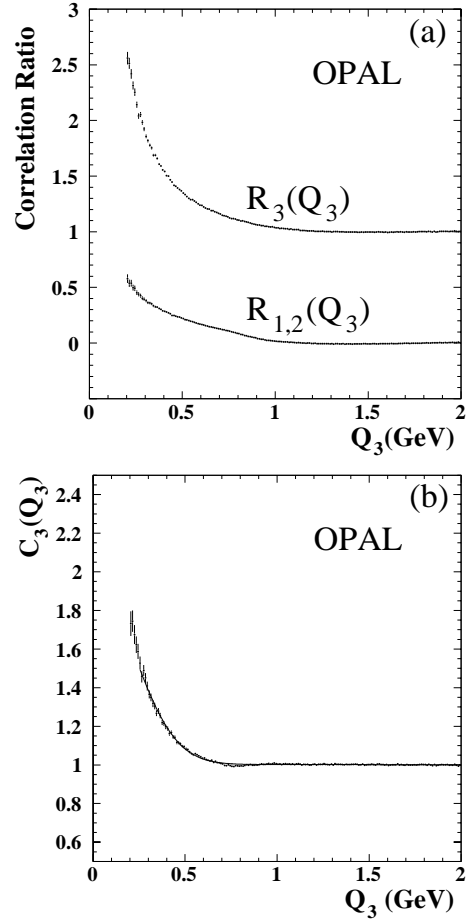


Fig. 1a,b. The $\pi^\pm\pi^\pm\pi^\pm$ BEC measured distributions, without Coulomb correction, as a function of Q_3 . **a** the measured $R_3(Q_3)$ and $R_{1,2}(Q_3)$ distributions before subtraction of the two-pion BEC, **b** the $C_3(Q_3)$ distribution after the subtraction of the two-pion BEC. These measurements are represented by points with statistical error bars. The solid line in **b** represents the fit result of (11), in the range $0.25 < Q_3 < 2.0$ GeV, to the measured $C_3(Q_3)$ distribution

5.1 The extraction of the genuine three-pion BEC

To extract the genuine three-pion BEC one has to subtract from $R_3(Q_3)$ the contribution coming from the well known two-pion BEC. In our analysis this last contribution is evaluated from the mixed-charged $\pi^\pm\pi^\pm\pi^\mp$ combinations of the data. To this end, it is convenient to rewrite $R_3(Q_3)$ as follows:

$$\begin{aligned} R_3(Q_3) &= \frac{N^{\pm\pm\pm}(Q_3)}{M^{\pm\pm\pm}(Q_3)} = 1 + \frac{N^{\pm\pm\pm}(Q_3) - M^{\pm\pm\pm}(Q_3)}{M^{\pm\pm\pm}(Q_3)} \\ &= 1 + \frac{\delta^{\pm\pm\pm}(Q_3)}{M^{\pm\pm\pm}(Q_3)}. \end{aligned} \quad (16)$$

The total excess $\delta^{\pm\pm\pm}(Q_3)$ above the Monte Carlo expectation has two contributions. The first from the two-pion BEC, $\delta_2^{\pm\pm\pm}(Q_3)$, and the second from the genuine three-pion BEC, $\delta_{\text{genuine}}^{\pm\pm\pm}(Q_3)$, so that:

$$\delta^{\pm\pm\pm}(Q_3) = \delta_2^{\pm\pm\pm}(Q_3) + \delta_{\text{genuine}}^{\pm\pm\pm}(Q_3). \quad (17)$$

From this it follows that what should be subtracted from $R_3(Q_3)$ to obtain the genuine three-pion BEC, is:

$$R_{1,2}(Q_3) = \frac{\delta_2^{\pm\pm\pm}(Q_3)}{M^{\pm\pm\pm}(Q_3)}. \quad (18)$$

Because we utilise for the subtraction the same events used for the $R_3(Q_3)$ measurement, there exists in every event with given charged multiplicity m and charge balance $\Delta = |n^+ - n^-|$ values a relation between $\delta_2^{\pm\pm\pm}(Q_3)$ and $\delta^{\pm\pm\mp}(Q_3) = N^{\pm\pm\mp}(Q_3) - M^{\pm\pm\mp}(Q_3)$. Here $N^{\pm\pm\mp}(Q_3)$ is the number of $\pi^\pm\pi^\pm\pi^\mp$ combinations in the data and $M^{\pm\pm\mp}(Q_3)$ is the corresponding number of combinations for the MC generated sample properly normalised to the data in the Q_3 range of 1.6 – 2.0 GeV.

If we define $n^{\pm\pm\mp}$ as the number of $\pi^\pm\pi^\pm\pi^\mp$ combinations in a given event, then it can be related to $n^{\pm\pm\pm}$, the number of $\pi^\pm\pi^\pm\pi^\pm$ combinations. A straightforward combinatorial calculation yields that for an event with given m and Δ values, one has:

$$\frac{n^{\pm\pm\mp}}{n^{\pm\pm\pm}} = 3 \left(1 + 4 \frac{m - \Delta^2}{m^2 - 4m + 3\Delta^2} \right). \quad (19)$$

In our analysis we utilise, after the application of the appropriate cuts, all the hadronic Z^0 decays lying within a wide range of multiplicity and charge balance. If we define $\langle n^{\pm\pm\pm}/n^{\pm\pm\mp} \rangle$ as the ratio $n^{\pm\pm\pm}/n^{\pm\pm\mp}$ averaged over all multiplicity and charge balance values in our data, then:

$$\int \delta_2^{\pm\pm\pm}(Q_3) dQ_3 = \left\langle \frac{n^{\pm\pm\pm}}{n^{\pm\pm\mp}} \right\rangle \times \int \delta^{\pm\pm\mp}(Q_3) dQ_3. \quad (20)$$

The integrations are carried out over the Q_3 region where $\delta_2^{\pm\pm\pm}(Q_3)$ and $\delta^{\pm\pm\mp}(Q_3)$ are different from zero. We further verified from MC studies that, to a good approximation, relation (20) holds also in its differential form, that is:

$$\delta_2^{\pm\pm\pm}(Q_3) = \left\langle \frac{n^{\pm\pm\pm}}{n^{\pm\pm\mp}} \right\rangle \times \delta^{\pm\pm\mp}(Q_3). \quad (21)$$

The average $\langle n^{\pm\pm\pm}/n^{\pm\pm\mp} \rangle$ depends on the multiplicity m and the charge balance Δ distributions of the data sample. Using the MC hadronic Z^0 decay sample we determined, by counting the number of combinations in the Q_3 range of 1.6 – 2.0 GeV, that $\langle n^{\pm\pm\mp}/n^{\pm\pm\pm} \rangle = 3.69$ with a negligible statistical error. The same value is obtained when the MC sample is replaced by the data sample. This value shifts to 3.71 when the Q_3 range is enlarged to 1.5 – 2.0 GeV. We also studied the variation of this ratio on the pion purity. To this end we evaluated this ratio from the MC sample using only tracks which were generated as pions with the result that $\langle n^{\pm\pm\mp}/n^{\pm\pm\pm} \rangle = 3.70$. The effect of the shift from 3.69 to 3.71 on the BEC parameters was found to be negligible in comparison to the statistical errors and to other systematic uncertainties (see Table 2).

In Fig. 2 we show the $\delta^{\pm\pm\pm}(Q_3)$ and the $\langle n^{\pm\pm\pm}/n^{\pm\pm\mp} \rangle \times \delta^{\pm\pm\mp}(Q_3)$ distributions as a function of Q_3 . As can be seen, the two distributions are similar in the higher Q_3

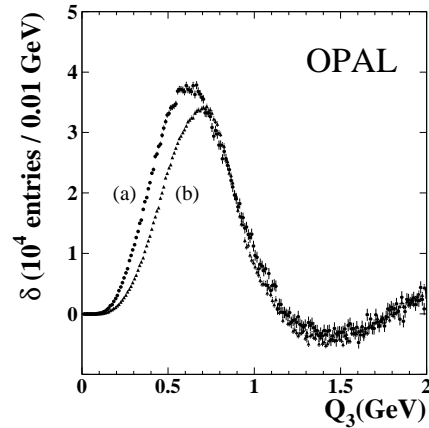


Fig. 2. **a** $\delta^{\pm\pm\pm}(Q_3)$ and **b** $\langle n^{\pm\pm\pm}/n^{\pm\pm\mp} \rangle \times \delta^{\pm\pm\mp}(Q_3)$ as functions of Q_3 . The errors plotted are the statistical ones. The difference between the distributions **a** and **b**, in the range $Q_3 < 0.7$ GeV, is due to the genuine three-pion BEC

Table 1. Results of the fit of (11) to the measured $C_3(Q_3)$ distributions without (Fig. 1b) and with (Fig. 4b) Coulomb correction carried out over the range of $0.25 < Q_3 < 2.0$ GeV. The fitted values are the genuine three-pion emitter r_3 and the BEC strength λ_3 together with the long range correlation parameter ε and the normalisation factor κ . The errors are the statistical ones obtained by the fits, and $\rho_{\lambda,r}$ is the correlation factor between λ_3 and r_3 . The quality of the fits are presented by their $\chi^2/\text{d.o.f.}$ values

Parameter	Without Coulomb Corr.	With Coulomb Corr.
λ_3	0.462 ± 0.012	0.504 ± 0.010
r_3 [fm]	0.616 ± 0.005	0.580 ± 0.004
κ	1.003 ± 0.001	1.026 ± 0.001
ε [GeV $^{-1}$]	-0.001 ± 0.001	-0.015 ± 0.001
$\rho_{\lambda,r}$	+0.887	+0.883
$\chi^2/\text{d.o.f.}$	218/171	190/171

region, namely between 0.7 and 2.0 GeV. The slight difference between the two distributions can be attributed to the systematic uncertainties given in Table 2, in particular those listed as items (f) and (g). Thus in this Q_3 range the excess of $\pi^\pm\pi^\pm\pi^\pm$ combinations is fully accounted for by the excess seen in the $\pi^\pm\pi^\pm\pi^\mp$ due to the two-pion BEC. In the lower Q_3 region an excess of $\delta^{\pm\pm\pm}(Q_3)$ over $\langle n^{\pm\pm\pm}/n^{\pm\pm\mp} \rangle \times \delta^{\pm\pm\mp}(Q_3)$ is observed which can no longer be attributed to the two-pion BEC and is therefore identified as the genuine three-pion BEC contribution, $\delta_{\text{genuine}}^{\pm\pm\pm}(Q_3)$. Thus:

$$C_3(Q_3) = R_3(Q_3) - R_{1,2}(Q_3) \quad (22)$$

$$= \frac{N^{\pm\pm\pm}(Q_3)}{M^{\pm\pm\pm}(Q_3)} - \frac{\delta^{\pm\pm\mp}(Q_3)}{M^{\pm\pm\pm}(Q_3)} \times \left\langle \frac{n^{\pm\pm\pm}}{n^{\pm\pm\mp}} \right\rangle.$$

In the present analysis we have used (23) to subtract the contributions due to the two-pion BEC.

The measured distribution $R_{1,2}(Q_3)$ is shown in Fig. 1a and the resulting $C_3(Q_3)$ distribution is shown in Fig. 1b, where a significant genuine three-pion BEC enhancement

is clearly present. The solid line in Fig. 1b represents the fit result of (11) to the data. The fitted values of λ_3 and r_3 and the correlation factor $\rho_{\lambda,r}$ are given in Table 1 together with the χ^2 value divided by the number of degrees of freedom (d.o.f.).

5.2 Evaluation of the Coulomb effect

The Coulomb correction to the genuine BEC, defined as $G_3(Q_3)$ in (14), can be applied either to the data or to the MC reference sample. These two possibilities are not expected to yield identical results since, unlike the MC generated sample, the data are affected by both the BEC and the Coulomb interactions. In our BEC analysis we chose to apply the Coulomb correction to the data and utilised the results coming from the second possibility as a measure of the systematic errors.

The Coulomb correction was accounted for by assigning to every three-pion combination of the data a weight equal to $1/(G_2(q_{1,2})G_2(q_{2,3})G_2(q_{1,3}))$. This automatically assures that $G_3(Q_3)$, defined in (14), is averaged only over all accessible experimental values of $q_{i,j}$. Using this procedure, the Coulomb correction factor $1/G_3(Q_3)$ can be evaluated at every Q_3 bin separately for the $\pi^\pm\pi^\pm\pi^\pm$ and the $\pi^\pm\pi^\pm\pi^\mp$ data samples. These correction factors are shown in Fig. 3a as a function of Q_3 in the range from 0.25 to 2.0 GeV. The resulting Coulomb correction applied to $C_3(Q_3)$, due to the corrections to $R_3(Q_3)$ and $R_{1,2}(Q_3)$, is shown in Fig. 3b where it is seen to rise as Q_3 decreases, reaching the value of about 11% at $Q_3 = 0.25$ GeV.

5.3 The corrected $\pi^\pm\pi^\pm\pi^\pm$ BEC distributions

The Coulomb corrected distributions $R_3(Q_3)$, $R_{1,2}(Q_3)$ and $C_3(Q_3)$ of the three-pion BEC, are shown in Fig. 4. A clear genuine three-pion Bose-Einstein enhancement is present in the low Q_3 region, from about $Q_3 = 0.7$ GeV reaching a value of $C_3(Q_3) = 2.0$ at $Q_3 = 0.2$ GeV. The continuous line in the figure represents the fit result of $C_3(Q_3)$ in the range $0.25 < Q_3 < 2.0$ GeV, as parametrised in (11). The quality of this fit, given by a $\chi^2/\text{d.o.f.} = 190/171$, represents an improvement over the fit result obtained for the Coulomb uncorrected $C_3(Q_3)$ distribution. The values obtained from the fit are $r_3 = 0.580 \pm 0.004$ fm for the emitter radius and a strength of $\lambda_3 = 0.504 \pm 0.010$, with correlation factor of $\rho_{\lambda,r} = +0.883$. These are listed in Table 1 together with the fit results for κ and ε . A comparison between the results presented in the table shows, as expected, that the value of λ_3 increases when the Coulomb correction is applied. We found that λ_3 increased by about 9% whereas r_3 decreased by about 6%.

5.4 Systematic errors

To estimate the systematic errors we have considered the effects on the λ_3 and r_3 results arising from the choice of

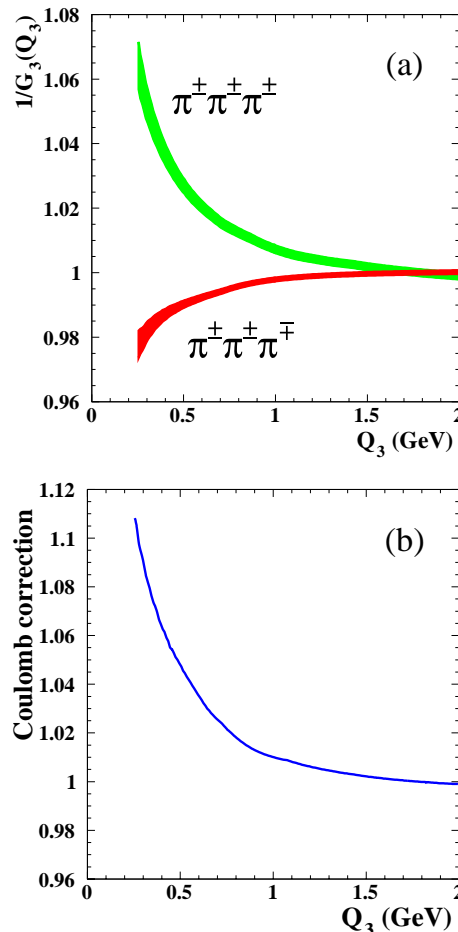


Fig. 3. **a** The Coulomb correction factors as a function of Q_3 for the $\pi^\pm\pi^\pm\pi^\pm$ and for the $\pi^\pm\pi^\pm\pi^\mp$ distributions. The width of the bands corresponds to the statistical uncertainty, **b** The mean net Coulomb correction value as a function of Q_3 for the genuine three-pion BEC distribution obtained by dividing the corrected $C_3(Q_3)$ distribution by the uncorrected one

the data selection criteria and from the procedure adopted for the Coulomb correction. We also investigated the effect on the results from our choice of the fitting range and the MC reference sample. These are summarised in Table 2.

In order to estimate the systematic effects related to track and event selection the analysis was repeated restricting the track selection criteria described in Sect. 4.2. To evaluate the possible contribution from our choice to account for the Coulomb effect on the BEC we also applied the Coulomb correction to the MC reference sample rather than to the data. Furthermore we considered for the fit two alternative Q_3 ranges. We also investigated the influence of adding a quadratic Q_3 term to the long range correlations. Finally, the systematic uncertainty coming from our choice of the JETSET 7.4 MC reference sample has been estimated by repeating the analysis with the HERWIG 5.8 [28] generated sample. This alternative MC uses a totally different model of fragmentation (cluster fragmentation) from that used by JETSET 7.4 (string formation and fragmentation). An estimate of the over-

Table 2. Results of several fits of the $C_3(Q_3)$ parametrisation to the data given with their statistical errors. The differences, $\Delta\lambda_3$ and Δr_3 , between the parameter values of the reference fit (a) and the others from (b) to (g) are added in quadrature to obtain an estimate of the combined systematic uncertainty associated with the fitted λ_3 and r_3 values. These are given in the last row

Fit variation	λ_3	$\Delta\lambda_3$	r_3 [fm]	Δr_3 [fm]
a. The reference fit	0.504 ± 0.010	—	0.580 ± 0.004	—
b. varying data selection cuts	0.519 ± 0.017	+0.015	0.561 ± 0.007	-0.019
c. MC Coulomb correction	0.488 ± 0.011	-0.016	0.586 ± 0.004	+0.006
d. fit range $0.25 < Q_3 < 1.5$ GeV	0.507 ± 0.011	+0.003	0.582 ± 0.005	+0.002
e. fit range $0.30 < Q_3 < 2.0$ GeV	0.471 ± 0.011	-0.033	0.569 ± 0.005	-0.011
f. addition of a long range Q_3^2 term	0.506 ± 0.010	+0.002	0.582 ± 0.004	+0.002
g. varying the MC reference sample	0.496 ± 0.026	-0.008	0.597 ± 0.015	+0.017
Total systematic error	—	0.041	—	0.029

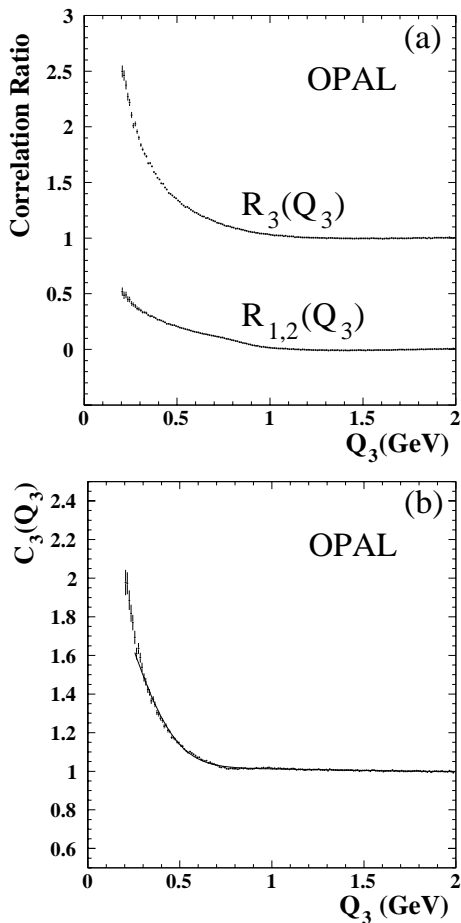


Fig. 4a,b. The Coulomb corrected $\pi^\pm\pi^\pm\pi^\pm$ BEC correlation distributions. **a** The non-subtracted $R_3(Q_3)$ and $R_{1,2}(Q_3)$ distributions, **b** the genuine $C_3(Q_3)$ distribution. The solid line in **b** represents the fit results of (11) over the range $0.25 < Q_3 < 2.0$ GeV

all systematic uncertainties was obtained by summing in quadrature the differences between each fit (b)–(g) and the reference fit (a).

The largest contributions to the over-all systematic error come from the choice of the selection criteria and from the choice of the lower Q_3 fit range limit. As seen in Table 2, the results for r_3 and λ_3 change by less than 4% when the Coulomb correction is applied to the Monte Carlo generated sample. We observe that λ_3 is rather sensitive to the choice of the lower Q_3 limit used as compared to the change of r_3 . In addition to the list given in Table 2, we also investigated other possible sources of systematic effects, such as the choice of the Q_3 bin size used in the fit, and verified that they indeed have negligible contributions. Finally, as noted above, the influence of the uncertainties of the ratio $\langle n^{\pm\pm\mp}/n^{\pm\pm\pm} \rangle$ on the subtraction formula and the fit results is also negligible.

Thus the final values of the BEC parameters are: $r_3 = 0.580 \pm 0.004$ (stat.) ± 0.029 (syst.) fm and $\lambda_3 = 0.504 \pm 0.010$ (stat.) ± 0.041 (syst.), where the uncertainties of the measured parameters are strongly dominated by the systematic errors. In Fig. 5 the 68% and 95% confidence level correlation contours for the BEC parameters are shown. The shape of the contours is determined mostly from the systematic errors. Accounting for the three-pion purity of 0.713 ± 0.053 , the BEC strength amounts to $\lambda_3^{\text{pure}} = 0.707 \pm 0.014$ (stat.) ± 0.078 (syst.) for a 100% pure $\pi^\pm\pi^\pm\pi^\pm$ system. The purity error of 0.053, due to the uncertainty of the MC generation rates, is incorporated in the systematic error of the λ_3^{pure} value.

6 Relation to other experimental results

A relation between the two-pion and three-pion emitter radii is derived in [9] based on the Fourier transform of the source distribution which is assumed to be of a Gaussian shape. This relation confines the emitter range \tilde{r}_3 as determined from a fit to $R_3(Q_3)$:

$$r_2/\sqrt{3} \leq \tilde{r}_3 \leq r_2/\sqrt{2}, \quad (23)$$

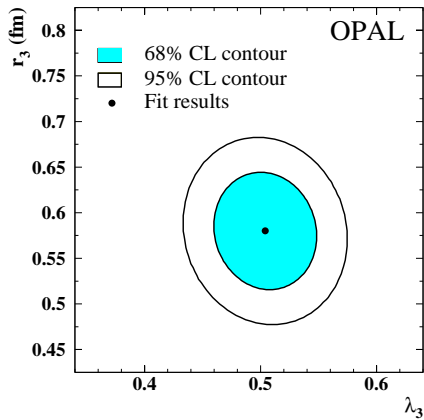


Fig. 5. The 68% and 95% confidence level correlation contours for the genuine three-pion BEC parameters λ_3 and r_3 after Coulomb correction. The contours are calculated from the statistical errors and the systematic uncertainties listed in Table 2. The best values are represented by the solid circle

where r_2 is the two-boson BEC emitter size. Since in our analysis the emitter radius is determined from the genuine BEC distribution $C_3(Q_3)$, the previous bounds reduce to the equality:

$$r_3 = r_2/\sqrt{2}. \quad (24)$$

In a former OPAL analysis [15], of the two-pion BEC present in the hadronic Z^0 decays, two options were adopted for the reference sample. The first utilised the correlations of the pairs of $\pi^+\pi^-$ in the data and the second used the two-pion correlations of Monte Carlo generated sample. Since in our analysis the reference samples were taken from the Monte Carlo generated events, we have checked relation (24) with the previously measured OPAL value, obtained by the second method, of $r_2 = 0.793 \pm 0.015$ fm, where only the statistical error was given. From (24) it follows that this r_2 value corresponds to $r_3^{\text{calc}} = 0.561 \pm 0.011$ fm, which is in good agreement with our value obtained from a fit to the data of $r_3 = 0.580 \pm 0.004$ (stat.) ± 0.029 (syst.) fm.

The BEC of the $\pi^\pm\pi^\pm\pi^\pm$ system has also been studied by the DELPHI collaboration [13] using the hadronic Z^0 decays measured at LEP. In that analysis, which neglected the Coulomb correction, the following results were obtained: $r_3 = 0.657 \pm 0.039$ (stat.) ± 0.032 (syst.) fm and $\lambda_3 = 0.28 \pm 0.05$ (stat.) ± 0.07 (syst.). The relatively large statistical errors reflect the fact that a much smaller data sample was used than in the present measurement. Our result for r_3 , before Coulomb correction, of 0.616 fm with a statistical error of ± 0.005 fm, is smaller than the DELPHI result but is consistent with it within one standard deviation. The measured λ_3 value depends on the pion track purity of the hadron sample analysed, so that caution has to be exercised when comparing the BEC strength values of different experiments. Keeping this in mind, we note that our mean λ_3 value lies considerably above that reported by DELPHI but it is still consistent with it within two standard deviations when the systematic errors are included.

7 Summary and conclusions

The Bose-Einstein correlations of three identical charged pions, produced in hadronic Z^0 decays, have been studied after correcting for the Coulomb interaction. A significant genuine three-pion Bose-Einstein correlation signal is observed near threshold in the $C_3(Q_3)$ distribution obtained after the subtraction of the two-pion correlation contribution. The radius r_3 of the three-pion emitter and the BEC strength λ_3 are measured to be:

$$r_3 = 0.580 \pm 0.004 \text{ (stat.)} \pm 0.029 \text{ (syst.) fm} \quad \text{and} \\ \lambda_3 = 0.504 \pm 0.010 \text{ (stat.)} \pm 0.041 \text{ (syst.)}$$

where the uncertainties are dominated by the systematic errors.

The Coulomb repulsive interaction opposes the Bose-Einstein enhancement in the low Q_3 region and therefore it is reasonable that in our analysis the Coulomb correction increased the λ_3 value. This increase amounts to about 9%. On the other hand, the Coulomb correction has a smaller effect on the r_3 value which is lowered by about 6%. Accounting for the three-pion purity the BEC strength amounts to $\lambda_3^{\text{pure}} = 0.707 \pm 0.014$ (stat.) ± 0.078 (syst.) for a 100% pure $\pi^\pm\pi^\pm\pi^\pm$ system.

A relation between the two-pion and the three-pion emitter dimensions was discussed in reference [9]. We tested this relation by using the present result and that obtained in the latest OPAL two-pion BEC analysis [15] where approximately the same data sample was used. The proposed relation between r_2 and r_3 , expressed in (24), is in good agreement with our results.

Acknowledgements. We particularly wish to thank the SL Division for the efficient operation of the LEP accelerator at all energies and for their continuing close cooperation with our experimental group. We thank our colleagues from CEA, DAPNIA/SPP, CE-Saclay for their efforts over the years on the time-of-flight and trigger systems which we continue to use. In addition to the support staff at our own institutions we are pleased to acknowledge the Department of Energy, USA, National Science Foundation, USA, Particle Physics and Astronomy Research Council, UK, Natural Sciences and Engineering Research Council, Canada, Israel Science Foundation, administered by the Israel Academy of Science and Humanities, Minerva Gesellschaft, Benozziyo Center for High Energy Physics, Japanese Ministry of Education, Science and Culture (the Monbusho) and a grant under the Monbusho International Science Research Program, German Israeli Bi-national Science Foundation (GIF), Bundesministerium für Bildung, Wissenschaft, Forschung und Technologie, Germany, National Research Council of Canada, Research Corporation, USA, Hungarian Foundation for Scientific Research, OTKA T-016660, T023793 and OTKA F-023259.

References

1. W.A. Zajc in *Hadronic Multiparticle Production*, (Ed. P. Carruthers), World Scientific, 1988, p. 235; S. Haywood,

- Where are we going with Bose-Einstein – A mini review, RAL Report 94-074
2. E.A. De Wolf, Bose-Einstein Correlations, Proc. XXVII Int. Conf. on High Energy physics, Glasgow, 20-27 July 1994 (Eds. P.J. Bussey and I.G. Knowles), Inst. of Physics Publ., 1995, p. 1281
 3. J. Ellis and K. Geiger, Phys. Rev. **D52** (1995) 1500; Phys. Rev. **D54** (1996) 1967
 4. B. Andersson and M. Ringnér, Nucl. Phys. **B513** (1998) 627
 5. L. Lönnblad and T. Sjöstrand, Phys. Lett. **B351** (1995) 293
 6. See e.g. E.A. De Wolf et al., Phys. Reports **270** (1996) 1
 7. TASSO Collab., M. Althoff et al., Z. Phys. **C30** (1986) 355; AFS Collab., T. Åkesson et al., Z. Phys. **C36** (1987) 517; LEBC-EHS Collab., M. Aguilar-Benitez et al., Z. Phys. **C54** (1992) 21
 8. Y.M. Liu et al., Phys. Rev. **C34** (1986) 1667
 9. I. Juricic et al., Phys. Rev. **D39** (1989) 1
 10. NA23 Collab., J.L. Bailly et al., Z. Phys. **C43** (1989) 341
 11. UA1 Minimum-Bias Collab., N. Neumeister et al., Phys. Lett. **B275** (1992) 186
 12. NA22 Collab., N.M. Agababyan et al., Z. Phys. **C68** (1995) 229
 13. DELPHI Collab., P. Abreu et al., Phys. Lett. **B355** (1995) 415
 14. OPAL Collab., P.D. Acton et al., Phys. Lett. **B267** (1991) 143
 15. OPAL Collab., G. Alexander et al., Z. Phys. **C72** (1996) 389
 16. G. Goldhaber et al., Phys. Rev. Lett. **3** (1959) 181; Phys. Rev. Lett. **120** (1960) 300
 17. M. Gyulassy et al., Phys. Rev. **C20** (1979) 2267
 18. M.G. Bowler, Phys. Lett. **B270** (1991) 69
 19. M. Biyajima et al., Phys. Lett. **B353** (1995) 340
 20. J.G. Cramer, Phys. Rev. **C43** (1991) 2798
 21. OPAL Collab., K. Ahmet et al., Nucl. Instr. Meth. **A305** (1991) 275; P. P. Allport et al., Nucl. Instr. Meth. **A324** (1993) 34; P. P. Allport et al., Nucl. Instr. Meth. **A346** (1994) 476
 22. M. Hauschild et al., Nucl. Instr. and Meth. **A314** (1992) 74
 23. O. Biebel et al., Nucl. Instr. and Meth. **A323** (1992) 169
 24. OPAL Collab., G. Alexander et al., Z. Phys. **C52** (1991) 175
 25. T. Sjöstrand, Comp. Phys. Comm. **39** (1986) 347; T. Sjöstrand and M. Bengtsson, Comp. Phys. Comm. **43** (1987) 367; T. Sjöstrand, Comp. Phys. Comm. **82** (1994) 74
 26. J. Allison et al., Nucl. Instr. and Meth. **A317** (1992) 47
 27. OPAL Collab., P. Acton et al., Z. Phys. **C58** (1993) 387; OPAL Collab., G. Alexander et al., Z. Phys. **C69** (1996) 543
 28. G. Marchesini et al., Comp. Phys. Comm. **67** (1992) 465